Influence of Plasticizers on Thermal and Mechanical Properties of Biocomposite Filaments made from Lignin and Polylactic Acid for 3D Printing

Sanjita Wasti[a], Eldon Triggs[b], Ramsis Farag[c,d], Maria Auad[c,d], Sushil Adhikari[a,e], Dilpreet Bajwa[f], Mi Li[g], Arthur J. Ragauskas[g,h,i]

[a] Department of Biosystems Engineering, Auburn University, Auburn, AL, USA
[b] Department of Aerospace Engineering, Auburn University, Auburn, AL, USA
[c] Department of Chemical Engineering, Auburn University, Auburn, AL, USA
[d] Center for Polymers and Advanced Composites, Auburn University, Auburn, AL, USA
[e] Center for Bioenergy and Bioproducts, Auburn University, Auburn, AL, USA
[f] Department of Mechanical and Industrial Engineering, Montana State University, Bozeman, MT, USA
[g] Center for Renewable Carbon, Department of Forestry, Wildlife and Fisheries, University of Tennessee, Knoxville, TN, USA
[h] Department of Chemical and Biomolecular Engineering, University of Tennessee, Knoxville, TN, USA
[i] Joint Institute for Biological Sciences, Biosciences Division Oak Ridge National Laboratory, Oak Ridge, TN, USA

Abstract

Polylactic acid (PLA) and organosolv lignin were mixed at different ratios and extruded to obtain PLA-lignin composite filaments. PLA was replaced with lignin up to 20 wt%. Two plasticizers (polyethylene glycol (PEG) 2000 and struktol TR451) were added in varying concentrations to enhance the properties of PLA_L20 (20% lignin in PLA) composite filaments. The effect of lignin in PLA, and PEG, and struktol in PLA_L20 composites was investigated via tensile test, differential scanning calorimetry, thermogravimetric analysis, scanning electron microscopy, Fourier transform infrared spectroscopy of the filaments, and dynamic mechanical analysis of 3D printed samples. A 2 wt% PEG was able to enhance both tensile stress and elongation at maximum load of PLA_L20 composite by 19% and 35%, respectively, whereas struktol TR451 was able to improve elongation at maximum load by 24%.

Keywords: PLA, lignin, biocomposites, thermal and mechanical properties, 3D printing.

1. Introduction

Additive manufacturing or 3D printing is a rapidly growing manufacturing technology that efficiently allows freeform fabrication of complex geometrical structures. Among different additive manufacturing technologies, fused deposition modeling (FDM) is the most popular and versatile technique in which a solid thermoplastic-filament is used as a feedstock [1]. The filament is passed through an extruder where it is melted, and material is deposited layer by layer in the build platform, solidifying to form a final object [2]. Commonly used thermoplastic polymers include polylactic acid (PLA), poly(ε-caprolactone) (PCL), ethylene-vinyl acetate (EVA), polyamides, high impact polystyrene (HIPS), and acrylonitrile butadiene styrene (ABS), and most of them are petroleum-based [2].

Petroleum-based polymers are extensively used in packaging, automobile industries, and construction [3]. The excessive use of these polymers has created environmental problems, such as the "plastic plague" and an increase in greenhouse gas emissions. To address environmental issues resulting from the excessive use of petroleum-based plastic and societies' transition from the single-use economy to a circular economy, researchers are developing bio-based sustainable materials that can be alternative to petroleum-based plastics.

PLA is the most commonly used thermoplastic biopolymer produced from glucose derived from corn-starch, sugarcane, and sugar beets [2–5]. It is a biodegradable and biocompatible polymer widely used for 3D printing applications primarily because of the lower glass transition and melting temperature compared to common thermoplastic polymers used for 3D printing and its non-adherence to printing surfaces [4,6,7,8]. Despite useful features, its brittle nature, low toughness, moisture sensitivity, and comparatively higher cost limit its broader applications [3,6]. On the other hand, lignin is the second most abundant biomaterial after cellulose. It is available in relatively large amounts as a byproduct from pulp and paper and potentially from the 2nd generation bioethanol industries [9–11]. A large portion of annually produced lignin is burnt to generate energy [9]. Due to lignin's heterogeneous-complex structure, and properties like low-purity standard, odor, and color issues, and the need for some form of physical and chemical modifications before its use, only 2% of annually produced lignin is used for preparing carbon fibers, chemicals, adhesives, plastics, and composites. However, most of those applications still lack successful commercialization [6,9,12].

Blending PLA with lignin to produce composite filaments for 3D printing is a promising bio-based option that could increase lignin utilization other than burning for energy. The use of lignin as a feedstock in the biopolymer manufacturing helps its valorization. Additionally, incorporating lignin in PLA decreases its (PLA) amount being used and reduces filaments' overall cost. It was found that adding 15wt% rice straw (US$ 0.28/kg) in ABS filament decreased the overall cost of the filament production that included additional processing costs [13]. Several studies were carried out regarding incorporating lignin in the PLA matrix to form composite filaments for 3D printing making it evident that lignin's addition often leads to a decrease in tensile strength and elongation [3,6,9]. Filaments with poor properties will be the death of successful commercialization efforts. There is still a lack of studies done regarding the enhancement of PLA-lignin composite filaments' properties. Various strategies were found from literature to be applied for enhancing the properties of polymer-lignin composite filaments, such as modifying lignin, adding plasticizers, and carbon fibers [1,12,14].

In this study, organosolv lignin was blended with the PLA in varying amounts to obtain composite filaments. We were successfully able to incorporate 20 wt% lignin in the composite filament. Beyond 20 wt%, the filaments were too brittle and could not be coiled around the spool. The thermal, mechanical, and morphological properties of produced composite filaments were studied. On observing the results, adding 20 wt% lignin in PLA showed poor mechanical properties even though we successfully produced filaments. Therefore, two different plasticizers (polyethylene glycol-PEG 2000 and struktol® TR451) were added in varying amounts in the PLA-20 wt% lignin mixture. PEG is a non-toxic, biodegradable plasticizer that makes the processability of polymer easier [15]. Struktol TR451 is a commercial plasticizer made up of oleochemicals and generally used in polymers to increase the filler content. It was found that both PEG and struktol TR451 were used to improve the processability and properties of PLA based composites [15,16]. The thermal, mechanical, and morphological properties of the composites were examined to determine plasticizers' effect. The central hypothesis of this study is that plasticizer can improve the mechanical properties of PLA-lignin composite filaments by preventing lignin agglomeration.

2. Materials and methods

2.1. Materials

PLA pellets (commercial grade: Ingeo 2003D) were purchased from Jamplast Inc. (Ellisville, MO, USA). Organosolv lignin (hardwood) was supplied by Attis Innovations, LLC (Milton, GA, USA). PEG 2000 was obtained from ThermoFisher Scientific Chemicals, Inc. (Waltham, MA, USA), whereas struktol® TR451 was supplied by Struktol Company of America, LLC (Stow, OH, USA).

2.2. Sample preparation

PLA pellets and lignin were oven-dried at 50 ℃ for more than 24 h before extruding the filaments. The composition of the filaments that were prepared in this study is presented in Table 1. PLA pellets and lignin were first manually mixed before feeding into the twin extruder (Leistritz Mic 18/GL 40D, Nuremberg, Germany). The twin-screw extruder had seven temperature zones, and they were set as follows from zone 1 to 7: 154 ℃, 157 ℃, 165 ℃, 170 ℃, 175 ℃, 178 ℃, and 178 ℃, respectively. The screw speed was set at 50 rpm. The filaments obtained were of varying diameters ranging from 1.30 mm to 2.10 mm, coiled around the filament spool, and stored in zip-lock bags before characterization.

{Insert Table 1 here}

2.3. 3D printing of filaments

A 3D cad model of dynamic mechanical analysis (DMA) samples of dimension 40 mm × 10 mm × 2 mm, and a dog bone sample according to ASTM D638 type V was prepared first using Autodesk Fusion 360. The files were then converted into .STL format. Ultimaker Cura 4.2.1 slicing software was used to slice the 3D model, and the gcode files were prepared. Filaments with a diameter in the range of 1.6 to 1.9 mm were selected and used for 3D printing using Monoprice MP Select Mini 3D Printer V2 (Monoprice Inc., Rancho Cucamonga, CA, USA). The printer had a nozzle diameter of 0.4 mm. The nozzle temperature of the printer was set at 210℃, whereas the bed temperature was set at 60℃ and the samples were printed with the print speed of 30mm/s

2.4. Lignin characterization

2.4.1. Proximate analysis

The proximate analysis includes the determination of moisture, volatile matter, ash, and fixed carbon content. The moisture content of lignin was determined according to the ASTM E871 using the Mettler Toledo moisture analyzer (Columbus, OH, USA). Volatile matter and ash content were determined according to the ASTM E872 and E1755, respectively. Finally, the fixed carbon was calculated by subtracting moisture, volatile matter, and ash content from 100.

2.4.2. Ultimate analysis

Total C, H, N, and S content of lignin was determined using a Vario micro elemental analyzer (Elementar Americas Inc, Ronkonkoma, NY, USA). Three replicates of lignin samples were prepared, and average values of C, H, N, and S content were reported.

2.4.3. Particle size

From the mortar and pestle ground lignin sample, 50 g was used to determine the particle size distribution using a Camsizer (Retsch Technology, Jenoptik, Germany).

2.5. Gel permeation chromatographic (GPC) analysis

GPC measured the weight-average molecular weight (M_w) and number-average molecular weight (M_n) of PLA and lignin according to a previously published method [17]. The filaments were manually cut into 1-2 mm pieces, allowing them to dissolve in tetrahydrofuran (THF) at ~1 mg/mL with stirring for 24 h. The resultant solution was filtered through a 0.45 μm membrane filter before GPC analysis. The size-exclusion separation was performed on an Agilent 1200 HPLC system (Agilent Technologies, Inc, Santa Clara, CA, US) equipped with Waters Styragel columns

(HR0.5, HR3, and HR5E; Waters Corporation, Milford, MA, US). A UV detector (270nm) was used for detection. THF was used as the mobile phase at a flow rate of 0.3 mL/min. Polystyrene narrow standards were used for establishing the calibration curve. PLA-lignin samples were measured in triplicate, and the average values were reported.

2.6. TGA

Thermogravimetric analysis (TGA) of all the samples was carried out by Q500 (TA Instruments, New Castle, DE, USA) under the nitrogen atmosphere at the flow rate of 60 mL/min. Samples of mass ranging from 7 to 13 mg were placed on the platinum pan and were heated from room temperature to 600 °C at the heating rate of 10 °C/min.

2.7. DSC

Differential Scanning Calorimetry (DSC) was performed using a Q 2000 (TA instruments, New Castle, DE, USA), operated under a nitrogen atmosphere at the flow rate of 50 mL/min. The samples, weighing from 4 to 6 mg, were first heated to 200 °C from room temperature at a heating rate of 10 °C/min and then were cooled from 200 °C to 40 °C at a cooling rate of 10 °C/min.

2.8. DMA

Viscoelastic properties of the 3D printed composites were studied using an RSA 3 (TA instruments, New Castle, DE, USA) under three-point bending mode. Dynamic temperature ramp test was performed over a temperature range from 25 ℃ to 100 ℃ at a ramp rate of 5 ℃/min, frequency of 1 Hz, and strain of 0.3%. Three specimens for each composition were tested, and average values were reported.

2.9. Mechanical testing

Mechanical properties of filaments were measured using an Instron 5565 (Norwood, MA, USA) with load cell 1 kN. The gauge length was fixed at 50 mm, and cross-head speed was set at 5 mm/min. The tensile test was carried out on 15 specimens for each composition, and average values were reported.

2.10. FTIR

Fourier transform infrared spectroscopy (FTIR) analysis of the samples was carried out using a Nicolet 6700 FTIR (ThermoFisher Scientific, Madison, WI, USA). Two spectra were collected in the wavelength range from 400-4000 cm^{-1} for each sample, and the average spectrum was reported. Each spectrum was recorded for a total of 64 scans with a resolution of 4 cm^{-1}.

2.11. SEM

Scanning Electron Microscopy (SEM) was used to study the cross-section of cryogenically fractured filaments and mechanically tested 3D printed samples using a Zeiss EVO50 (Carl Zeiss Microscopy, NY, USA). Liquid nitrogen was used to fracture the filaments. As the specimens were non-conductive, they were gold-sputtered using an EMS 150R ES (Electron Microscopy Sciences, PA, USA) sputtering system. The surface was studied at a different magnification at an accelerating voltage of 15 kV and a working distance of approximately 8 mm to 10.5 mm.

2.12. Statistical analysis

Statistical analyses were performed using SAS 9.4 (Cary, NC, USA). Analysis of variance (ANOVA) was carried out to evaluate the effect on mechanical properties upon the addition of lignin and plasticizers in PLA. All analyses were performed at 0.05 significance level (i.e. $\alpha = 0.05$).

3. Results and Discussion

3.1. Lignin characterization

3.1.1. Proximate analysis

The moisture, volatile matter, ash, and fixed carbon content of the lignin sample used for the experiment were found to be 1.39 ± 0.07 %, 78.25 ± 0.51%, 2.88 ± 0.27%, and 17.49 ± 0.61% (all on a mass basis), respectively. On comparing the moisture content among different lignin, Gordobil et al. [18] mentioned that the average moisture content of all types of lignin was in the range of 2-5%, which is nearly similar to the values obtained in our analysis. However, the values of volatile matter and fixed carbon content of the lignin used in this study had a more substantial variation than those mentioned by Gordobil et al. [18]. Gordobil et al. [18] found 63% of volatile matter and 33% of fixed carbon content in organosolv eucalyptus lignin. Furthermore, Gordobil et al. [18] found the ash content of organosolv eucalyptus lignin to be 3.6%, which was slightly higher than this study.

3.1.2. Ultimate analysis

With regards to the ultimate analysis of the lignin sample, the average carbon, hydrogen, nitrogen, and sulfur contents were found to be 65.70 ± 0.70%, 6.10 ± 0.05%, 0.15 ± 0.01%, and 0.30 ± 0.10%, respectively. Mimini et al. [3] also reported 62.3% of C, 6.28% of H, 0.29% of N, and <0.02% of S content in organosolv lignin used for blending with PLA, which is similar to our result of the ultimate analysis.

3.1.3. Particle size

From the Camsizer, the average particle size of the lignin sample was found to be 911µm. It was found that the particle size of the filler affects the composites' mechanical properties [19]. However, none of the research done on bio-composite filaments using lignin has mentioned the exact values or range of particle size of lignin for better filament processing.

3.2. GPC analysis

The number average molecular weight (Mn) and weight average molecular weight (Mw) of the PLA filament was 62,345±540 g/mol and 121,153±2,556 g/mol, respectively. Backes et al. [20] mentioned Mn and Mw of 2003D PLA pellets to be 118,600 g/mol and 168,000 g/mol, which was higher than that obtained in this experiment. Organosolv lignin used for the experiment had Mn and Mw of 555±29 g/mol and 1,239±27 g/mol, respectively. This value of lignin's molecular weight was comparatively lower than the molecular weight of different lignin presented in Tolbert et al.[21]. Tolbert et al.[21] has presented that the source from which lignin was extracted and the process parameters used during organosolv pretreatment affects the molecular weight of lignin. On performing the GPC of the PLA_L20 composite, two different peaks were observed representing PLA and lignin's molecular weight, respectively. On quantifying the peaks, Mw and Mn of PLA and lignin in the composite were found to be 130,100±5,626 g/mol and 84,146±1,650 g/mol and, 1,090±15 g/mol and 678±14 g/mol, respectively.

3.3. TGA

Figures 1a and 1b show the TG and DTG curves of PLA, lignin, PLA_L20, PLA_L20_P1, PLA_L20_P2, and PLA_L20_S0.5, and PLA_L20_S1, respectively. From the TG curve of lignin, it was found that 36.62% of the lignin sample remained at 600 ℃, which was due to the formation of a highly condensed aromatic structure with the ability to form char [9,22]. The DTG graph of lignin reveals that weight loss of lignin has different stages. Different functional groups and structural elements present in lignin have different decomposition temperatures, which leads to the multistage degradation of lignin. A decrease in onset decomposition of PLA from 349 ℃ to 342 ℃ on adding 20 wt% lignin can be observed from the TG curve of PLA and PLA_L20 composite. This decrease in the onset decomposition temperature of PLA_L20 might be due to earlier decomposition of lignin present in the PLA matrix. However, there was no change in the maximum degradation temperature on adding lignin. It was also found that at 600 ℃, there was an increase in residue to 7% with the addition of 20 wt% lignin.

Furthermore, with the addition of 1% PEG in PLA_L20, there was no change in the TG curve of PLA_L20. On further increasing PEG content to 2- 5wt%, there was a decrease in the maximum decomposition temperature from 371 ℃ to 345℃. Li et al. [15] observed a similar decrease in PLA's maximum degradation temperature with the addition of PEG. Likewise, with the addition of up to 1wt% struktol in PLA_L20, there was no notable change in the TG curve, which was due to the lower concentration of struktol added.

{Insert Figure 1 here}

3.4. DSC

The DSC results of PLA, PLA-lignin, and PLA-lignin plasticizer composites are presented in Table 2, whereas the heating and cooling cycle of PLA is shown in Figure 2. The heating cycle gives the three characteristics features: glass transition, cold crystallization, and melting temperature, while the cooling cycle provides the crystallization peak that determines the crystalline nature of materials. At 10 ℃/min cooling rate, no significant crystallization peaks were found in the case of PLA as well as PLA composites.

From the obtained results, neat PLA showed the Tg of 59 ℃, which decreased to 53 ℃ on incorporating 20 wt% of lignin. This result implies that on adding 20 wt% lignin in PLA, PLA shows soft and rubbery properties at a lower temperature than neat PLA. The decrease in Tg with the addition of lignin was due to the modification of molecular mobility of the PLA matrix on adding lignin[23]. However, there was no noticeable change in Tg of PLA-lignin composites on adding PEG and struktol. This effect might be because of the low concentration of incorporated PEG and struktol.

There are several factors, such as spatial confinement, nucleation on sample boundaries, temperature gradient, and melt flow, affecting crystallization [3]. The crystallization rate is also affected by adding fillers like lignin in the PLA matrix. These additional phases (i.e., lignin) either assist or hinder the chain mobility and thus affect crystallization [3]. With the addition of 20wt% lignin, the cold crystallization temperature (Tcc) of PLA decreases from 121 ℃ to 113 ℃, which means that crystallization occurs at a lower temperature than neat PLA. Mimini et al. [3] observed the decrease in Tcc from 130 ℃ to 120 ℃ and 115 ℃ upon adding kraft lignin and lignosulfonate in the PLA matrix, respectively. Tcc of PLA_L20 further decreased to 107 ℃ and 109 ℃ on adding 5 wt% PEG and 1 wt% struktol, respectively. This decrease in Tcc was basically due to an increase in chain mobility [15]. Similarly, on adding 20 wt% lignin, the melting temperature of PLA-lignin composite decreased from 150℃ to 146 ℃. This decrease in Tg and Tm represents the probable interaction between the PLA and lignin since the phenolic hydroxyl group of lignin

can form intermolecular hydrogen bonds with the carbonyl group of PLA [24]. However, there was no change in the melting temperature of PLA_L20 composite with the addition of PEG and struktol.

{Insert Figure 2 and Table 2 here}

3.5. DMA

Storage or dynamic modulus (E') indicates the stiffness of the material and represents the ability of the material to store the applied energy [25]. The variation in E' as a function of temperature for PLA, PLA_L20, PLA_L20_P2, PLA_L20_P5, PLA_L20_S0.5, and PLA_L20_S1 composites are shown in Figure 3a. The E' of PLA_L20 composite was higher than that of PLA, implying that the PLA's stiffness increases on adding lignin. It was found that with the addition of PEG in PLA_L20 composite, there was a decrease in E'. The rigidity and stiffness of PLA_L20 composite decrease due to the plasticizing effect of PEG and the flexibility of the molecular chain. Guo et al. [26] found a similar decrease in storage modulus upon adding epoxidized soybean oil in PLA-succinylated lignin-epoxidized soybean oil composites. There was also a decrease in E' upon addition of struktol to 1 wt% in PLA_L20 composite, which might also be due to the plasticization effect of struktol.

Tan δ is the mechanical damping factor or loss factor and is represented as a loss modulus to storage modulus ratio. From Figure 3b, it can be noted that with the increase in temperature, the tan δ value increases until it reaches Tg and then decreases. Typically, the maximum tan δ value is observed at Tg. The high value of tan δ represents the non-elastic nature of the material, whereas the lower value represents the elasticity [25]. From Figure 3b, a slight shift in Tg to the lower temperature with the addition of 20 wt% of lignin can be observed, which is due to poor dispersion of lignin particles in the PLA matrix,can be seen in SEM images. Again, from Figure 3b, a decrease in the value of tan δ with the addition of 2wt% PEG can be observed, which represents the elastic nature of composite. This effect was basically due to the plasticizing effect of PEG and improvement in the dispersion of lignin particles in the PLA matrix. However, there was an increase in the value of tan δ on further increasing PEG to 5 wt%, which is probably due to the presence of void, as seen in SEM images, see section 3.8 . Furthermore, there was no notable shift in glass transition temperature with the addition of PEG. From Figure 3b, a slight decrease in the value of tan δ as compared to that of PLA_L20 was observed on adding struktol on varying concentrations. This outcome was probably due to the non-uniform dispersion of lignin on adding struktol.

On comparing the Tg values between the one obtained from DSC and DMA, the value of Tg obtained from DMA is comparatively higher than that obtained from DSC. Since Tg represents a thermodynamic transition, its value for

the same material depends on several factors, such as measurement technique, sample geometry, and anisotropy [27]. Furthermore, 3D printed samples' anisotropic nature is the reason behind the difference in values obtained among DMA and DSC [27].

Loss modulus (E") is the material's ability to dissipate applied energy. It represents the viscous response of the material. E" is sensitive to different molecular motions, transition, morphology, and structural heterogeneities [25]. The curves of PLA, PLA-lignin, and PLA-lignin-plasticizer composites are presented in Figure 3c. At room temperature, it was found that neat PLA had lower E" than other composites. This result represented that there was a change in polymer motion [26]. An increase in lignin content resulted in an increase in the molecular friction, which might be the reason for higher E" of PLA-lignin composites.

{Insert Figure 3 here}

3.6. Mechanical testing

The results of mechanical testing of PLA, PLA_L20, PLA_L20_P2, PLA_L20_P5, PLA_L20_S0.5, and PLA_L20_S1 are presented in Figure 4. This data shows that with the addition of lignin in PLA, the tensile strength of the composite decreases. There is a 25% decrease in tensile strength with a 20 wt% addition of lignin. The statistical analysis found that tensile stress at the maximum load of PLA decreased significantly upon adding 10, 15, and 20 wt% of lignin. This result was attributed to a decrease in the effective load-bearing cross-section of PLA in the presence of lignin [28]. With the increase in the lignin amount, the size of the lignin aggregates get larger, as can be seen in SEM images, see section 3.8. This was due to the coalescence of the lignin particles [6]. The larger the filler size, the smaller the surface area to volume ratio, which results in smaller interfacial area and stress transfer to the matrix-filler interface. Besides this, poor interfacial adhesion between lignin aggregates and PLA matrix might have affected the stress transfer between the matrix and filler. Anwer et al. [23] also found a decrease in tensile strength with the increase in filler size and filler content in the polymer matrix. Similarly, there was a significant decrease in elongation at the maximum load from 4.14 to 2.94% on adding 20 wt% lignin to the PLA matrix. Spiridon et al.[29] also observed a 50% decrease in elongation of PLA on adding 15 wt% lignin and explained that the decline might be due to H-bonding and polar interaction between PLA and lignin particles, which restricted the ductile flow. On the contrary, tensile modulus increased from 1.93 to 2.26 GPa on adding 20wt% lignin to the PLA matrix, which was possibly due to the constraint exerted by the lignin on the PLA matrix [29].

The tensile stress at maximum load of PLA_L20 increased from 42.90 MPa to 50.84 MPa (nearly by 19%) on adding 2 wt% PEG. The tensile stress at maximum load decreased to 42.39 MPa on increasing PEG content to 5wt%. On applying Tukey's HSD test for multiple comparisons, it was found that the concentration of PEG from 0.75-4 wt% in PLA_L20 composite had significant improvement in tensile stress at maximum load when compared with PLA_L20 ($p<0.05$). However, there was still a significant difference in tensile stress at max. load between PLA and PLA_L20_P2 by 11%. There are several factors behind this difference in strength, such as filler matrix interaction, filler size, and phase separation. From SEM images of the PLA_L20_P2 composite, well-dispersed lignin particles of reduced particle size in the PLA matrix can be observed. The smaller the particle size, the larger the interfacial area, and the larger the stress transfer to the matrix-filler interface. This effect was one of the reasons for the increase in the tensile strength of the PLA_L20 composite with the addition of 2wt% PEG. Besides that, the probable hydrogen bond between PLA and PEG [15] and PEG and lignin [30] might have improved the adhesion between phases, which thus resulted in improved strength of the composite. However, the reason behind the decrease in strength with an increase in PEG to 5wt% was the voids in the fracture surface, which had probably occurred due to the accumulation of PEG during phase separation. The elongation at maximum load of PLA_L20, on the other hand, was significantly increased from 2.94 to 3.98% on adding 2 wt% PEG, which was basically due to the decrease in the tensile modulus of the composite on adding PEG. Chieng et al. [31] also found the inversely proportional relationship between the tensile modulus and elongation. Adding 2-5 wt% PEG in the PLA_L20 composite had a similar elongation at max. load as that of neat PLA. There was a decrease in the tensile modulus of PLA_L20 on the addition of PEG, and the value was similar to that of neat PLA. Gordobil et al.[32] found a similar decrease in modulus with the addition of plasticizer.

On adding struktol, a commercial plasticizer, there was a slight increase in tensile stress at max load. PLA_L20_S0.25 showed a maximum increase in tensile stress at max. load of PLA_L20 from 42.90 to 45.88 MPa (nearly by 7%). On performing Tukey's HSD test for multiple comparisons on the obtained results of tensile stress of PLA-lignin- struktol composites, it was found that there was no significant improvement in tensile stress at max. load of the PLA_L20 composite upon adding struktol until 1 wt% ($p>0.05$). However, the elongation at maximum load was increased significantly by 24% on adding 0.5 wt% struktol in the PLA_L20 composite. On adding struktol above this, there was a decrease in elongation at max. load of PLA_L20. On the other hand, as expected, the tensile modulus of PLA_L20 decreased on adding the struktol plasticizer. Moreover, the tensile modulus of PLA_L20 with varying concentrations of struktol had no significant difference than that of neat PLA.

{Insert Figure 4 here}

3.7. FTIR

The FTIR spectra of PLA and PLA-lignin composites are presented in Figure 5. From the FTIR spectrum of neat PLA, a strong absorption band near 1746 cm^{-1} is seen, attributed to C=O stretching of the carbonyl group. The Lignin spectrum had similar IR absorption near this region, but the peak intensity is weaker as compared to that of PLA. In the spectrum of PLA, peaks at 1450 cm^{-1}, 1380 cm^{-1}, and 1360 cm^{-1} were attributed to CH_3 anti-symmetric bending vibration, deformation, and symmetric mode of the CH group, respectively, whereas the signal near 2996 cm^{-1} was due to stretching of the CH_3 group. O-H stretching of the hydroxyl groups of lignin yielded a strong absorption band near 3400 cm^{-1} [28]. On adding lignin in the PLA matrix, there was a slight increase in peak intensity at 3450 cm^{-1}. This result might be because of hydrogen bonds forming between the phenolic hydroxyl groups of lignin and carbonyl groups of PLA [24,28]. A small peak at 1515 cm^{-1} can be seen in the PLA_L20 composite, which might have attributed by C=C groups of aromatic rings of lignin[9]. Since the amount of PEG and struktol added was in small quantities, there were no notable changes in spectra.

{Insert Figure 5 here}

3.8. SEM

The SEM image of the cross-section of cryogenically fractured neat PLA filament (Figure 6a) appears smooth with little plastic deformation representing a brittle failure. With the increase of lignin content, lignin particles' size enlarges due to lignin aggregates (Figure 6b and 6c). Nguyen et al. observed similar enlargement in lignin particle size with an increase in lignin content [1]. On adding PEG in PLA_L20 composite, the particle size of lignin was significantly reduced, and lignin particles were well dispersed in the PLA matrix. This reduced lignin size was due to PEG which prevented lignin from coalescence to form lignin aggregates. The dispersion of lignin profoundly influenced the mechanical properties of PLA-lignin composites.. There was an increase in ductile fibrils with the increase in PEG content at 2 wt% (in Figure 6d), which represented equal dispersion of PEG particles in the PLA matrix and increased in elongation at maximum load [33]. On further increasing PEG content to 5 wt%, there were observable voids in the fractured surface, probably due to PEG accumulation during phase separation (Figure 6e). Similar ductile fibrils and voids were observed by Sungsanit et al. [33] on varying PEG content in the PLA matrix.

On observing the SEM image of the PLA_L20_S1 composite (Figure 6f), it was found that there was no significant decrease in lignin particle size as compared to that in PLA_L20_P2 composite. Also, the distribution of lignin particles

in the PLA matrix was not improved on adding struktol. The cryogenically fractured surface had a short fibrillary structure, which represents the ductile failure in nature. This result may be the reason behind the slight improvement in elongation at maximum load on adding 1 wt% struktol in PLA_L20.

{Insert Figure 6 here}

3D printing of dog bone samples prepared using PLA_L20_P2 composite filaments was used (Figure 7a) to investigate the 3D printing behavior and print quality. It was found that the nature of the filament diameter and its consistency played a crucial role in the sample's print quality, its mechanical properties, and dimensional accuracy. It was found that the region printed with lower filament diameter had observable voids, pores, and missing layers, whereas the one printed with a diameter above 1.9 mm had a problem of over-extrusion. Over-extrusion was a major reason behind the poor shape and dimensional inaccuracy. On observing the SEM images of fractured dog bone samples (Figure 7b and 7c), it was found that there was good layer adhesion between two printed layers and no voids.

{Insert Figure 7 here}

4. Conclusions

Biocomposite filaments using PLA and lignin were developed, and their thermal, mechanical, and morphological properties were studied. It was found that upon 5 wt% addition of lignin, there was a significant drop in elongation at a maximum load; however, tensile strength was comparable to that of neat PLA. On further increasing the lignin content beyond 5wt%, there was a gradual decrease in tensile strength and elongation, whereas the tensile modulus and storage modulus increased. We demonstrated that 20 wt% PLA could be replaced with lignin while making filaments, but the filaments had degraded tensile properties. On increasing the lignin content above 25 wt.%, filaments obtained were brittle and did not have enough flexibility to be rolled in a filament spool.

It was found that 2 wt% addition of PEG in the PLA_L20 composite, the tensile strength, and elongation of PLA_L20 significantly increased by 19% and 35%, respectively. On the other hand, adding 0.5 wt% struktol in PLA_L20 significantly increased elongation by 24%. However, there was no significant improvement in tensile strength. Processing bio-composites showed good extrudability and printability. SEM images of the 3D printed specimen suggested the better adhesion between the layers with no observable voids. Even after adding the plasticizer in the PLA_L20 composites, tensile strength was still significantly lower than the neat PLA by 11%. Perhaps, the strength of the 3D printed parts can be improved by varying different 3D printing parameters.

Acknowledgments

This material is based upon work supported by the Alabama Agricultural Experiment Station and Hatch (ALA014-1-19068) program of the US Department of Agriculture National Institute of Food and Agriculture. Also, the authors would like to thank Auburn University Intramural Grant Program for their financial support and Attis Innovations, LLC for providing lignin samples free of charge for this work.

References

[1] Nguyen NA, Barnes SH, Bowland CC, Meek KM, Littrell KC, Keum JK, et al. A path for lignin valorization via additive manufacturing of high-performance sustainable composites with enhanced 3D printability. Sci Adv 2018;4:eaat4967. https://doi.org/10.1126/sciadv.aat4967.

[2] Wasti S, Adhikari S. Use of Biomaterials for 3D Printing by Fused Deposition Modeling Technique: A Review. Front Chem 2020;8:1–14. https://doi.org/10.3389/fchem.2020.00315.

[3] Mimini V, Sykacek E, Hashim SNA, Holzweber J, Hettegger H, Fackler K, et al. Compatibility of Kraft Lignin, Organosolv Lignin and Lignosulfonate With PLA in 3D Printing. J Wood Chem Technol 2019;39:14–30. https://doi.org/10.1080/02773813.2018.1488875.

[4] Cuiffo MA, Snyder J, Elliott AM, Romero N, Kannan S, Halada GP. Impact of the Fused Deposition (FDM) Printing Process on Polylactic Acid (PLA) Chemistry and Structure. Appl Sci 2017;7:579. https://doi.org/10.3390/app7060579.

[5] Gordobil O, Egüés I, Llano-Ponte R, Labidi J. Physicochemical properties of PLA lignin blends. Polym Degrad Stab 2014;108:330–8. https://doi.org/10.1016/j.polymdegradstab.2014.01.002.

[6] Gkartzou E, Koumoulos EP, Charitidis CA. Production and 3D printing processing of bio-based thermoplastic filament. Manuf Rev 2017;4:1. https://doi.org/10.1051/mfreview/2016020.

[7] Xu W, Pranovich A, Uppstu P, Wang X, Kronlund D, Hemming J, et al. Novel biorenewable composite of wood polysaccharide and polylactic acid for three dimensional printing. Carbohydr Polym 2018;187:51–8. https://doi.org/10.1016/j.carbpol.2018.01.069.

[8] Chiulan I, Frone A, Brandabur C, Panaitescu D. Recent Advances in 3D Printing of Aliphatic Polyesters. Bioengineering 2017;5:2. https://doi.org/10.3390/bioengineering5010002.

[9] Tanase-Opedal M, Espinosa E, Rodríguez A, Chinga-Carrasco G. Lignin: A biopolymer from forestry biomass for biocomposites and 3D printing. Materials (Basel) 2019;12:1–15.

https://doi.org/10.3390/ma12183006.

[10] Leão AL, Cesarino I, Dias OAT, Negrão DR, Gonçalves DFC. Recent approaches and future trends for lignin-based materials. Mol Cryst Liq Cryst 2017;655:204–23. https://doi.org/10.1080/15421406.2017.1360713.

[11] Kun D, Pukánszky B. Polymer/lignin blends: Interactions, properties, applications. Eur Polym J 2017;93:618–41. https://doi.org/10.1016/j.eurpolymj.2017.04.035.

[12] Nguyen NA, Bowland CC, Naskar AK. A general method to improve 3D-printability and inter-layer adhesion in lignin-based composites. Appl Mater Today 2018;12:138–52. https://doi.org/10.1016/j.apmt.2018.03.009.

[13] Osman MA, Atia MRA, Osman MA, Atia MRA. Investigation of ABS-rice straw composite feedstock fi lament for FDM. Rapid Prototyp J 2018;24:1067–75. https://doi.org/10.1108/RPJ-11-2017-0242.

[14] Akato K, Tran CD, Chen J, Naskar AK. Poly(ethylene oxide)-Assisted Macromolecular Self-Assembly of Lignin in ABS Matrix for Sustainable Composite Applications. ACS Sustain Chem Eng 2015;3:3070–6. https://doi.org/10.1021/acssuschemeng.5b00509.

[15] Li D, Jiang Y, Lv S, Liu X, Gu J, Chen Q, et al. Preparation of plasticized poly (lactic acid) and its influence on the properties of composite materials. PLoS One 2018;13:1–15. https://doi.org/10.1371/journal.pone.0193520.

[16] Mamun A Al, Nikousaleh MA, Feldmann M, Rüppel A, Sauer V, Kleinhans S, et al. Lignin Reinforcement in Bioplastic Composites. In: Faruk O, Sain M, editors. Lignin Polym. Compos., William Andrew Publishing; 2016, p. 153–65.

[17] Li M, Yoo CG, Pu Y, Biswal AK, Tolbert AK, Mohnen D, et al. Downregulation of pectin biosynthesis gene GAUT4 leads to reduced ferulate and lignin-carbohydrate cross-linking in switchgrass. Commun Biol 2019;2:1–11. https://doi.org/10.1038/s42003-018-0265-6.

[18] Gordobil O, Moriana R, Zhang L, Labidi J, Sevastyanova O. Assesment of technical lignins for uses in biofuels and biomaterials: Structure-related properties, proximate analysis and chemical modification. Ind Crops Prod 2016;83:155–65. https://doi.org/10.1016/j.indcrop.2015.12.048.

[19] Migneault S, Koubaa A, Erchiqui F, Chaala A, Englund K, Wolcott MP. Effects of processing method and fiber size on the structure and properties of wood-plastic composites. Compos Part A Appl Sci Manuf

2009;40:80–5. https://doi.org/10.1016/j.compositesa.2008.10.004.

[20] Backes EH, Pires DN, Costa LC, Passador FR, Pessan LA. Analysis of the Degradation During Melt Processing of PLA / Biosilicate ® Composites 2019.

[21] Tolbert A, Akinosho H, Khunsupat R, Naskar AK, Ragauskas AJ. Characterization and analysis of the molecular weight of lignin for biorefining studies. Biofuels, Bioprod Biorefining 2014;8:836–56. https://doi.org/10.1002/bbb.

[22] Watkins D, Nuruddin M, Hosur M, Tcherbi-Narteh A, Jeelani S. Extraction and characterization of lignin from different biomass resources. J Mater Res Technol 2015;4:26–32. https://doi.org/10.1016/j.jmrt.2014.10.009.

[23] Anwer MAS, Naguib HE, Celzard A, Fierro V. Comparison of the thermal, dynamic mechanical and morphological properties of PLA-Lignin & PLA-Tannin particulate green composites. Compos Part B Eng 2015;82:92–9. https://doi.org/10.1016/j.compositesb.2015.08.028.

[24] Li J, He Y, Inoue Y. Thermal and mechanical properties of biodegradable blends of poly(L-lactic acid) and lignin. Polym Int 2003:949–52. https://doi.org/10.1002/pi.1137.

[25] Saba N, Jawaid M, Alothman OY, Paridah MT. A review on dynamic mechanical properties of natural fibre reinforced polymer composites. Constr Build Mater 2016;106:149–59. https://doi.org/10.1016/j.conbuildmat.2015.12.075.

[26] Guo J, Wang J, He Y, Sun H, Chen X, Zheng Q, et al. Triply Biobased Thermoplastic Composites of Polylactide/Succinylated Lignin/Epoxidized Soybean Oil. Polymers (Basel) 2020;12.

[27] Idrees M, Jeelani S, Rangari V. Three-Dimensional-Printed Sustainable Biochar-Recycled PET Composites. ACS Sustain Chem Eng 2018;6:13940–8. https://doi.org/10.1021/acssuschemeng.8b02283.

[28] Kumar Singla R, Maiti SN, Ghosh AK. Crystallization, Morphological, and Mechanical Response of Poly(Lactic Acid)/Lignin-Based Biodegradable Composites. Polym - Plast Technol Eng 2016;55:475–85. https://doi.org/10.1080/03602559.2015.1098688.

[29] Spiridon I, Tanase CE. Design, characterization and preliminary biological evaluation of new lignin-PLA biocomposites. Int J Biol Macromol 2018;114:855–63. https://doi.org/10.1016/j.ijbiomac.2018.03.140.

[30] Mu L, Shi Y, Wang H, Zhu J. Lignin in Ethylene Glycol and Poly(ethylene glycol): Fortified Lubricants with Internal Hydrogen Bonding. ACS Sustain Chem Eng 2016;4:1840–9.

https://doi.org/10.1021/acssuschemeng.6b00049.

[31] Chieng BW, Ibrahim NA, Yunus WMZW, Hussein MZ. Plasticized poly(lactic acid) with low molecular weight poly(ethylene glycol): Mechanical, thermal, and morphology properties. J Appl Polym Sci 2013;130:4576–80. https://doi.org/10.1002/app.39742.

[32] Gordobil O, Egüés I, Labidi J. Modification of Eucalyptus and Spruce organosolv lignins with fatty acids to use as filler in PLA. React Funct Polym 2016;104:45–52. https://doi.org/10.1016/j.reactfunctpolym.2016.05.002.

[33] Sungsanit K, Kao N, Bhattacharya SN. Properties of Linear Poly(Lactic Acid)/Polyethylene Glycol Blends. Polym Eng Sci 2012:108–16. https://doi.org/10.1002/pen.

Figures captions

Figure 1: a) TG and b) DTG curves of different samples.

Figure 2: Heat and cooling cycle of PLA

Figure 3: a) Storage modulus, b) Loss factor, and c) Loss modulus of PLA, PLA-lignin, and PLA-lignin-plasticizer composites.

Figure 4: Mechanical properties of PLA, PLA-lignin and PLA-lignin-plasticizer composites

Figure 5: FTIR spectrum of PLA, lignin, and PLA_L20

Figure 6: SEM images of a) PLA, b) PLA_L10, c) PLA_L20, d) PLA_L20_P2, e) PLA_L20_P5 and f) PLA_L20_S1 composites (red arrows indicate lignin aggregates)

Figure 7: a) 3D printed dog bone sample, SEM images of b) fracture surface and c) side view of the dog bone sample prepared from PLA_L20_P2 filaments

Figures

Figure 1

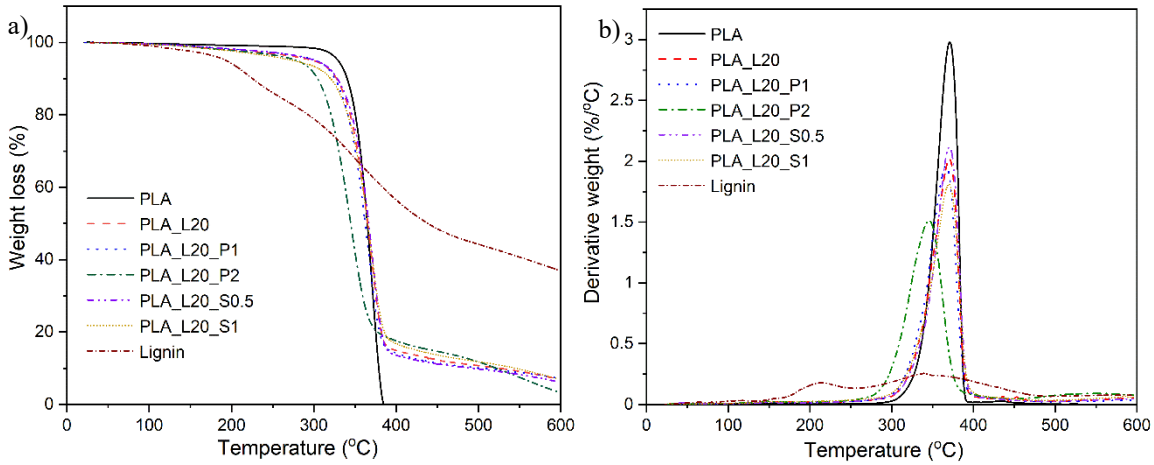

Figure 2

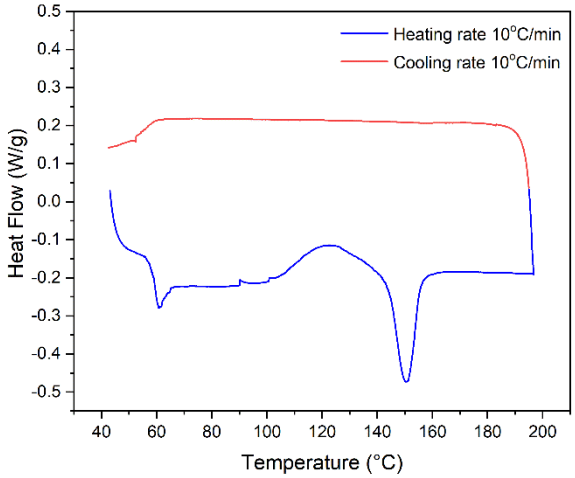

Figure 3

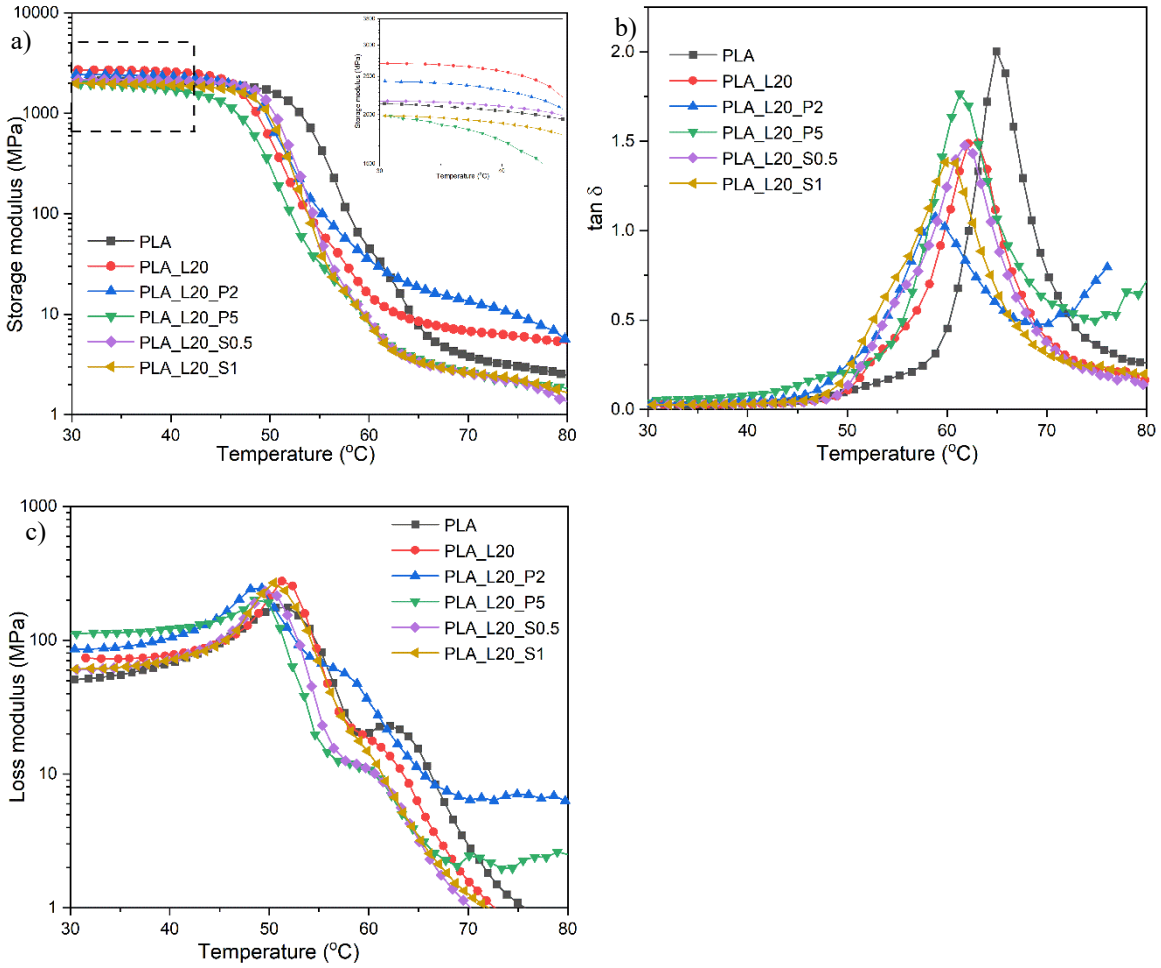

Figure 4

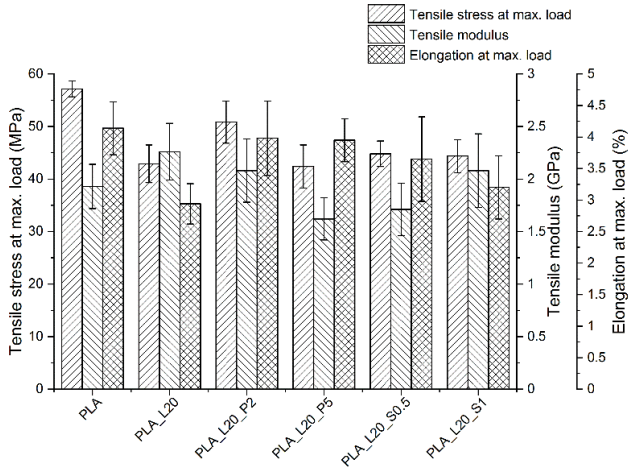

Figure 5

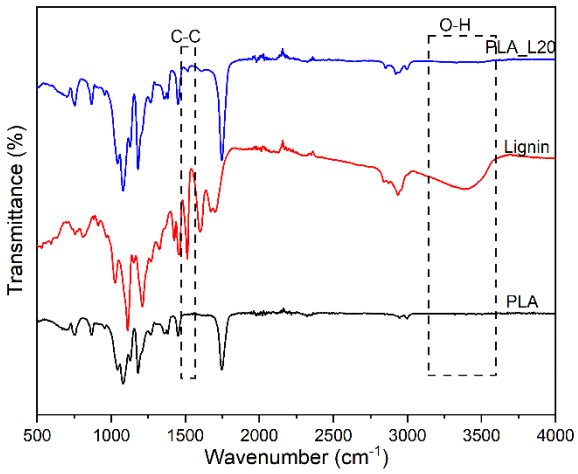

Figure 6

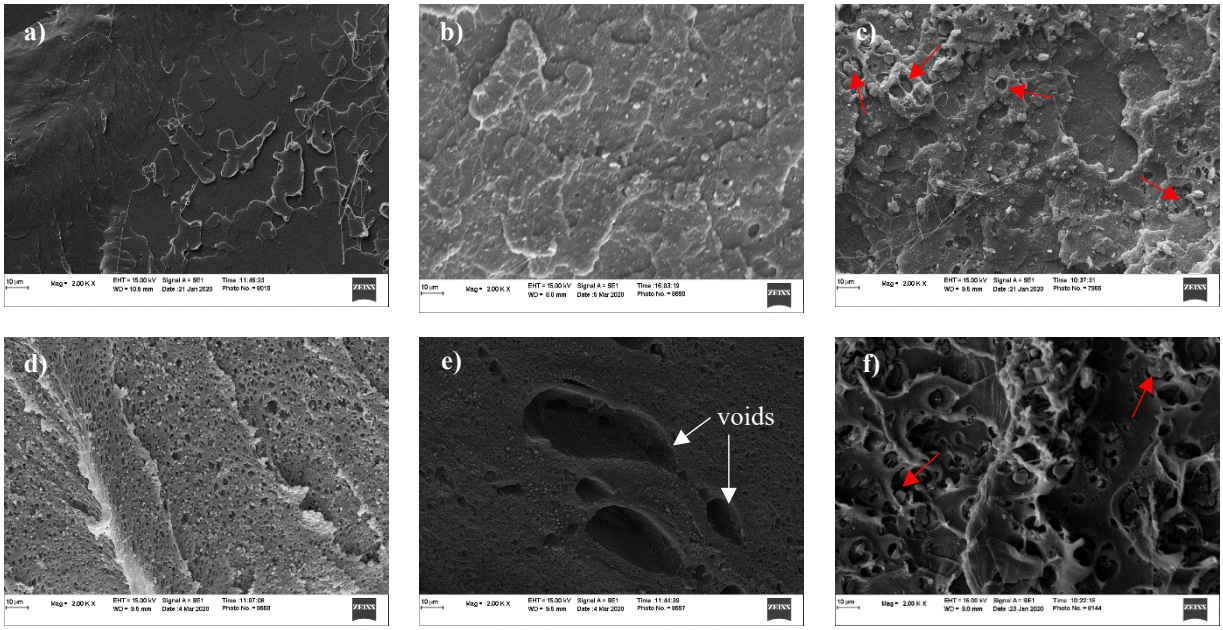

Figure 7

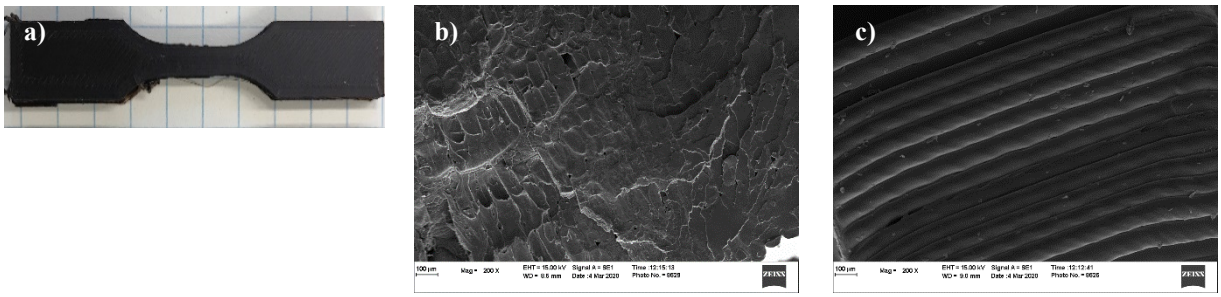

Table 1 Total samples prepared along with their sample codes

Sample code	PLA (wt%)	Lignin (wt%)	PEG (wt%)	Struktol (wt%)
PLA	100	-	-	-
PLA_L5	95	5	-	-
PLA_L10	90	10	-	-
PLA_L15	85	15	-	-
PLA_L20	80	20	-	-
PLA_L20_P0.25	79.75	20	0.25	-
PLA_L20_P0.5	79.50	20	0.50	-
PLA_L20_P0.75	79.25	20	0.75	-
PLA_L20_P1	79	20	1	-
PLA_L20_P2	78	20	2	-
PLA_L20_P3	77	20	3	-
PLA_L20_P4	76	20	4	-
PLA_L20_P5	75	20	5	-
PLA_L20_S0.25	79.75	20	-	0.25
PLA_L20_S0.5	79.50	20	-	0.50
PLA_L20_S0.75	79.25	20	-	0.75
PLA_L20_S1	79	20	-	1

Note: PLA- Polylactic acid, L- lignin, P- polyethylene glycol and S- struktol

Table 2: Transition temperatures and enthalpies of PLA and PLA-lignin composites

Sample	Tg (℃)	Tcc (℃)	Hcc (J/g)	Tm (℃)	Hm (J/g)
PLA	59.13	121.22	9.62	150.43	13.03
PLA_L20	52.57	112.91	9.19	145.65	14.33
PLA_L20_P2	52.71	106.30	12.50	143.78	22.46
PLA_L20_P5	51.49	107.21	11.15	145.83	15.05
PLA_L20_S0.5	51.51	108.24	13.17	142.81	18.97
PLA_L20_S1	51.02	108.90	11.31	145.97	15.35